DEM simulation of dry granular flow impacting a rigid wall

A. Albaba, S. Lambert & F. Nicot
Irstea de Grenoble - Unité ETNA, Saint Martin d'Hères, France
Adel.albaba@irstea.fr stephane.lambert@irstea.fr
francois.nicot@grenoble.cemagref.fr
and
B. Chareyre
Laboratoire Sols, Solides, Structures, Grenoble, France
bruno.chareyre@3sr-grenoble.fr

ABSTRACT

This study presents a model for simulating the impact behavior of dry granular flow against a rigid wall using Discrete Element Method (DEM). The simulations were carried out using poly-dispersed clumps consisting of two overlapping spherical particles accounting for the shape effects of gravel particles. The particles were flowing in an inclined flume where different inclination angles were tested and interaction forces with the wall were recorded. The model calibration was in particular based on particle shape and flow thickness measurements. Compared with the experimental results, the model showed good agreement regarding the peak impact force, the time of the peak force and the final (residual) force at the end of the tests.

INTRODUCTION

The rapid increase of urban activities in mountainous areas encouraged more attention to be given to the mitigation of threats caused by natural hazards such as rockfalls and debris flow. Due to their high flow velocity and impact forces, long runout distance and poor temporal predictability, granular flows have been classified as one of the most hazardous landslides (Jakob & Hungr 2005). However, their hazard can be mitigated by the use of protection structures similar in principle to rockfall barriers (Guasti et al. 2011). Such structures are either retaining walls (Kishi et al. 2000) or flexible structures made of nets (Nicot et al. 2001). The estimation of total impact force exerted by granular flows on such structures is an important factor in their design. Such a force generally varies with slope angle, thickness of the flowing material and velocity at the moment of the impact.
Numerical models of granular flows have been generally classified into continuum and discrete models. Continuum treatment has often been adopted where flows characteristics are

analyzed by the Eulerian forms of continuity and momentum equation (Azana et al. 1999). On the other hand, with the use of a Discrete Element Method (DEM), Silbert et al. (2001) carried out 2D and 3D simulations of mono-dispersed particles flowing in a steady-state condition where observations were taken regarding structure and rheology of the flow. Faug et al. (2009) proposed a hydrodynamic model based on depth-averaged momentum conservation which was used to predict DEM numerical results of a free-surface gravity-driven dense flow overflowing a wall. On the experimental side, a variety of experimental studies have been carried out ranging from studies on geological debris flows to well characterized laboratorial granular flows down an inclined plane (Azana et al. 1999). However, none of the experiments considered coarse-grained flow of angular particles which is the main case for actual dry granular flow.

The aim of this paper is to present a DEM-based model which is able to simulate the impact behavior of dry granular flow of angular particles against a rigid wall. First, we will describe the experimental data (Jiang & Towhata 2013) available for model calibration and validation. Next, we describe the model in terms of contact law, particles shape and flume characteristics. Afterwards, the model calibration and validation are presented with discussion of obtained results. Finally conclusions of the presented work are drawn.

EXPERIMENTAL DATA

Jiang & Towhata (2013) recently studied the impact behavior of dry granular flow against a rigid retaining wall using poly-dispersed mixture of limestone gravel. Particles were of a poly-dispersed gravel mixture ranging from 10 mm to 20 mm in diameter. The samples (which had specific weight of 13.5 kN/m^3) were prepared in a box with varying lengths (from 14 cm to 44 cm with a 5 cm step) and heights (from 5 cm to 20 cm with a 5 cm step) but with a 30 cm fixed width. The samples were released in a dam-break manner in which the gate was pulled instantaneously.

The flume was rectangular in cross section with 219 cm length, 30 cm width and 35 cm height. Different inclination angles α were tested ranging from 30˚ to 45˚. The friction angle of the flume base, flume sides and the rigid wall were 25˚, 15˚ and 21˚ respectively. At the end of the flume, a perpendicular rigid wall divided into six horizontal segments (marked from 1 to 6 starting from the bottom) was used. Interaction forces were recorded with each 5-cm in height segment of the wall.

Measurements of normal impact force vs. time were recorded along with observations of flow thickness and flow velocity at the time where the total normal force on the wall reaches its maximum. These experimental data were selected for our model calibration and validation. This is because it considers elongated coarse-grained flow of angular particles which is the main case for actual dry granular flow. In addition, the study provided detailed measurement of normal impact force for different heights (different segments of the rigid wall).Three different tests have been presented in the paper: Test L34-H15-α45^o, Test L44-H15-α40^o and Test L44-H20-α40^o. For instance, Test L44-H15-α40^o represents a sample having 44 cm in length, 15 cm in height and 40˚ inclination angle.

NUMERICAL MODEL

DEM has been used to carry out the simulation of the dry granular flow. Nowadays DEM is widely used for modeling granular media. It is particularly efficient for static and dynamic simulation of granular assemblies where medium can be described at a microscopic scale. The method is based on the molecular dynamics approach proposed by Cundall & Strack (1979).

Compared with Finite Element Method (FEM), DEM makes large displacements between elements easy to simulate. In addition, DEM surpasses FEM when dealing with discontinuous problems where FEM becomes computationally demanding. YADE software has been used as a modeling tool which is an extensible open-source framework for discrete numerical models, focused on Discrete Element Method (Šmilauer et al. 2010).

Contact law

A visco-elastic contact law with Mohr-coulomb failure criterion (Figure 1) has been adopted where normal and tangential contact forces F_n, F_t between particles were calculated as follows:

$$\vec{F_n} = (k_n u_n - \gamma \dot{u}_n)\vec{n} \tag{1}$$

$$\vec{F_t} = \begin{cases} \frac{k_t \vec{u_t}}{|k_t \vec{u_t}|} |\vec{F_n}| \tan\varphi & \text{if } |k_t \vec{u_t}| > |\vec{F_n}| \tan\varphi, \\ k_t \vec{u_t} & \text{otherwise} \end{cases} \tag{2}$$

where k_n and k_t are the normal and tangential stiffness parameters, u_n and u_t are the normal and shear displacements, $\tan\varphi$ is the friction coefficient and γ is the viscous damping coefficient. k_t was taken as (2/7) k_n as previously suggested by Silbert et al. (2001).

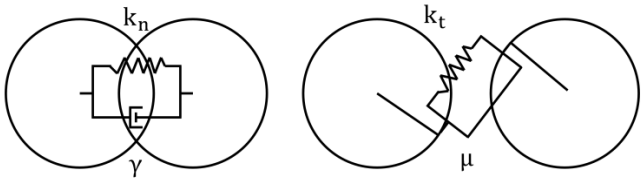

Figure 1. **Normal and tangential interaction forces of the contact**

Based on Schwager & Pöschel (2007), with the restitution coefficient (ε) being the ratio between velocities after and before the impact, $\varepsilon_{n,t}$ (normal and tangential) can be calculated as follows:

$$\beta_{n,t} = \frac{\gamma_{n,t}}{m} \tag{3}$$

$$\omega_{n,t} = \sqrt{\left(\frac{2k_{n,t}}{m_{eff}}\right)^2 - \beta^2} \tag{4}$$

$$\varepsilon_{n,t} = \frac{\dot{u}(t_c^0)}{\dot{u}(0)} = e^{-\beta\pi/\omega} \tag{5}$$

where $m_{eff} = (1/m_1 + 1/m_2)$, m_1 and m_2 are the masses of two interacting particles and $\dot{u}(t_c^0)$, $\dot{u}(0)$ are velocities after and before the collision respectively.

Contact law

Two shapes were compared: a simple spherical shape and a clump. The clump consists of two identical spheres (with a radius R) overlapping over a distance R thus having an aspect ratio of 3/2.

With the total weight of the sample being equal to the weight of a single D_{50}-sphere multiplied by the number of particles, the number of generated particles (num) was calculated as follows:

$$num = \left(\frac{V_t \gamma_t}{V_s \gamma_s}\right) \quad (6)$$

where V_t is the total volume of the sample, γ_t is the specific weight of the sample (13.5 kN/m^3), V_s is the volume of a single D_{50}-sphere and γ_s is the specific weight of gravel particles (taken as 26.5 kN/m^3 for the limestone gravel considered). Afterwards, each spherical particle was replaced with a clump consisting of two equal spheres. Radii of clumped-spheres were calculated so that the density and volume of the clump is equal to that of the particle which it replaces meaning that the overlapping volume is not counted twice.

MODEL CALIBRATION

The model calibration has been carried out considering the shape of the particles and the value of ε based on the flow thickness measurements. It is worth noting that, due to the absence of lubricated contact, the tangential viscous damping coefficient has been set to zero (i.e. ε_t = 1.0) as suggested by Ghaisas et al. (2004). Particle stiffness k_{par} = E D/2 where E is the Young's modulus (taken as 10^8 Pa) and D is the particle diameter. In order to ensure rigidity, the wall stiffness was taken ten times the stiffness of D_{50} particle. Friction angles of flume base, side walls and rigid wall were taken similar to values provided by the experimental data (Section 2). The model has been calibrated and validated for Test L34-H15-α45°, Test L44-H15-α40° and Test L44-H20-α40°. Results shown in the calibration section are for Test L44-H15-α40°.

Clumps vs. spherical particles

Two samples were tested: the first having spherical particles and the second having clumped ones. Clumps proved to be advantageous in lowering rotational energy (Figure 2a), adding interlocking effect between particles and improving shape representation of the angular gravel. Furthermore, the simulation is kept rather inexpensive (with the use of only two spheres for forming the clump).

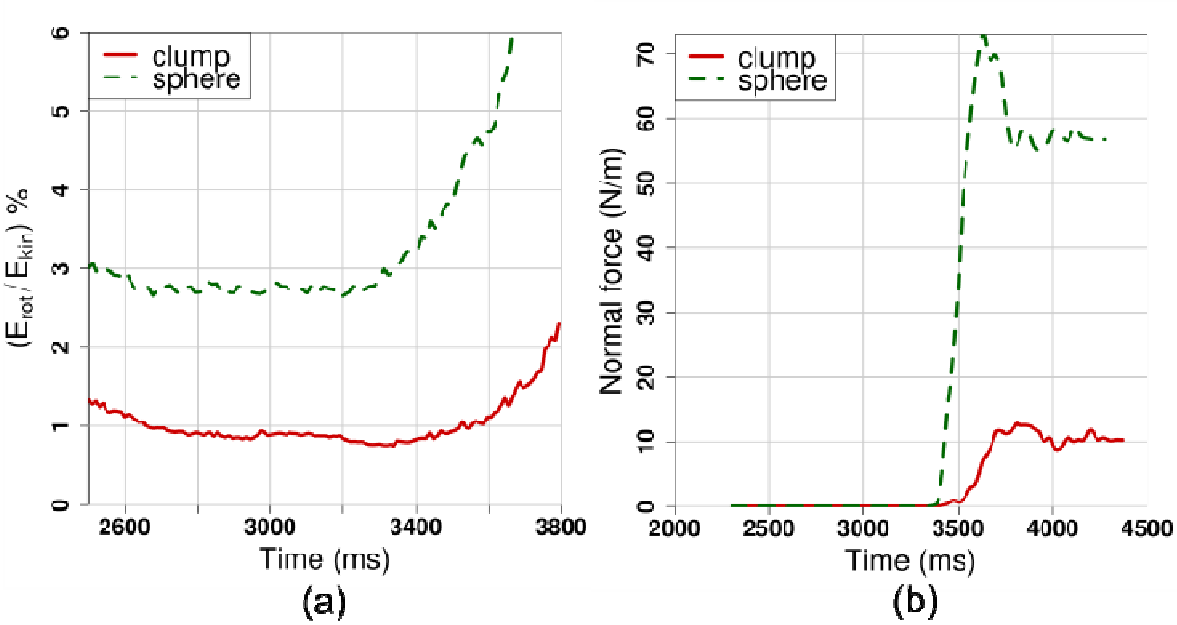

Figure 2. **Test L44-H15-α40°: (a) Ratio of rotational energy to total kinetic energy for clumps and spheres, (b) Normal force on part 6 of the wall**

Consequently, compared with the spherical particles, peak and residual values (Figure 2b) on the sixth segment of the wall for clumped particles are closer to the experimental (experimental values: $F_{peak} \approx 14$ N/m, $F_{res} \approx 10$ N/m). This might be due to the rolling resistance provided by the clump shape which prevents the particles from rolling over the dead zone deposit and accumulate behind part 6 of the wall. As a result, clumped particles are used for the rest of the tests as they proved superiority over spherical ones.

Flow thickness and velocity

The targeted part of the flow for calculating velocity and thickness were particles within a distance ranging from 40 to 50 cm away from the wall. However, since the flow has two regimes along the flow thickness-collisional and frictional-, cumulative frequency were drawn in which thickness and velocity values were taken at 90% of total frequency of particle center. A value of $D_{50}/2$ was added to 90% cumulative frequency of the flow thickness to account for the free surface of the flow.

Different values of restitution coefficient were tested and flow thickness values were observed for each corresponding restitution coefficient. It was found that $\varepsilon = 0.3$ is suitable for our flow based on flow thickness measurements resulting in a model value of 3.9 cm which well-correspond to the experimental value of 3.9 cm (Figure 3a).

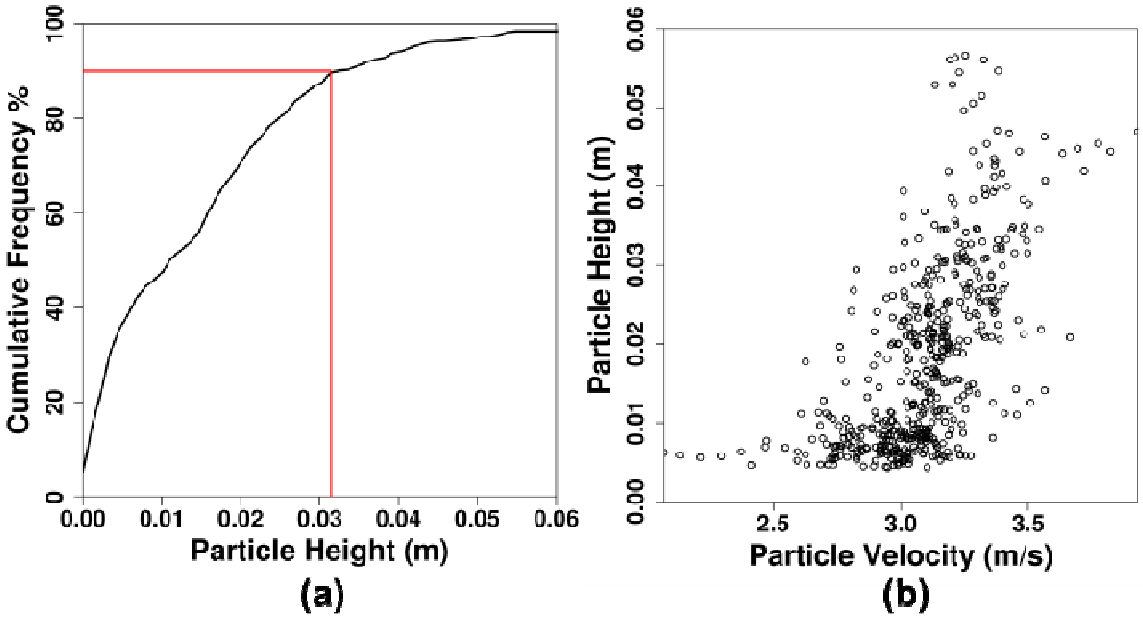

Figure 3. **Test L44-H15-α40°: (a) Cumulative frequency of gravity center of particles height, (b) Variation of particles velocity with heights**

However, velocity measurement of test L44-H15-α40° in the model (Figure 3b) taken at the considered flow thickness (at 90% for cumulative frequency) was found to be lower than experimental value (model: 3.33 m/s, exp: 4.13 m/s) which still needs further investigation. However, it is worth highlighting that measurements of velocity were taken only for the particles at the top surface of the flow.

MODEL VALIDATION

The rigid wall response against the granular flow impact has been investigated in details. Indeed, special attention has been given to the normal force applied on each part of the rigid wall where curves of normal impact force vs. time were analyzed. Due to the tendency of DEM results showing large fluctuation, a data treatment was needed. Data treatment was carried out using smooth spline method where a smooth curve is fitted to a set of noisy data using spline function. The advantages of using splines are their computationally speed and simplicity, as well as the clarity of controlling curvature directly (Chambers & Hastie 1992).

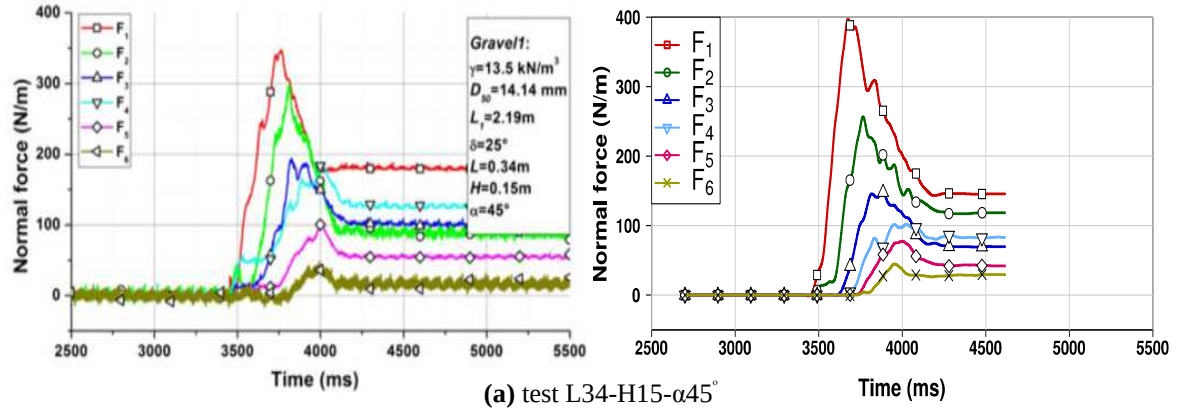

(a) test L34-H15-α45°

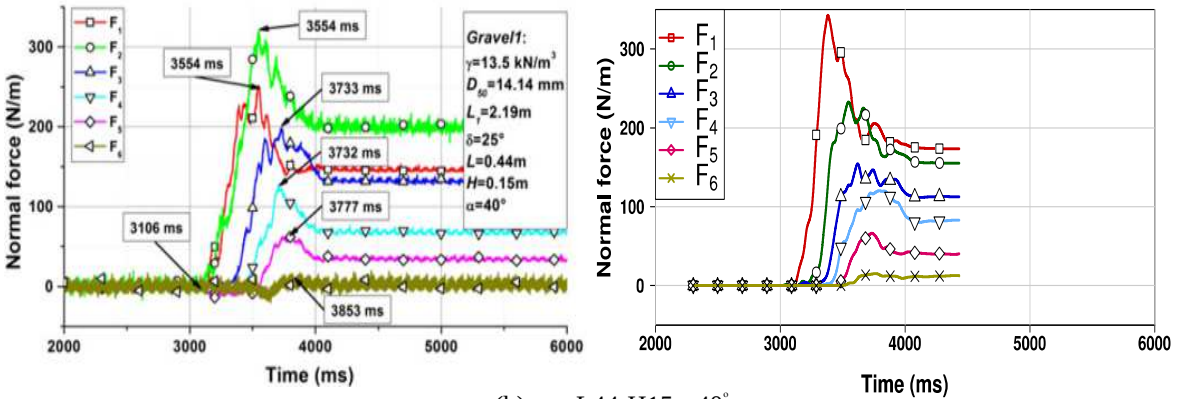

(b) test L44-H15-α40°

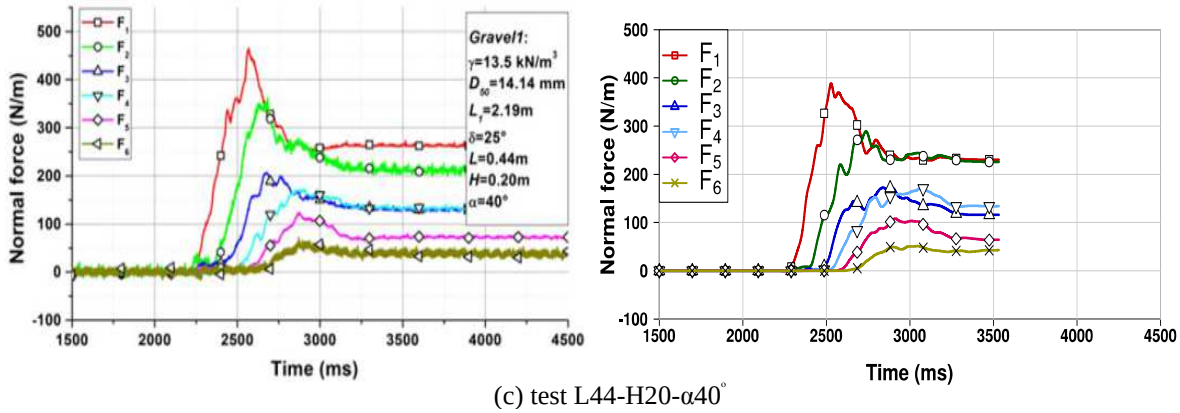

(c) test L44-H20-α40°

Figure 4. **Time history of normal force variation: model (right) and experiment (Jiang & Towhata 2013) (left)**

Test L34-H15-α45°

In this test (Figure 4a), for the first element of the wall (F_1), the peak force was found to be 396 N/per wall width which is fairly close to the experimental value (around 350 N/m). Moreover, the time of the peak force F_1 is relatively similar to the experiment with a value around 3676 ms but with a lower residual force in the model (145 N/m) compared with the experiment (175 N/m). Likewise, in contrast to F_1, the peak value of F_2 in the model (256 N/m) was lower than the experimental value (300 N/m). For F_3 and F_4, the model captured the

peak time of forces fairly well (being 3883 and 3994 ms for F_3 and F_4 respectively) but with a lower peak value. The peak force and timing of the peak on F_5 and F_6 were fairly captured by the model along with their residual force values.

Test L44-H15-α40˚

For this test, the peak impact force values were 341 and 232 N/m for F_1 and F_2 respectively (Figure 4b). Compared to the experiment, similar values were observed but with a reversed order ($F_2 > F_1$). Concerning the rest of the wall, the model managed to capture the peak forces of F_3, F_4, F_5 and F_6 (with a small exception for F_3) with values of 154, 120, 66 and 15 N/m respectively along with peak times 3619, 3808, 3733 and 3761 ms respectively. Residual forces on these parts were found to be 112, 82, 40 and 12 N/m respectively which are close to the experimental observations.

Test L44-H20-α40˚

With the use of higher volume of the sample, the trend of the impact force curves was better captured with the model along with the time lag between each force curve. For instance, F_1 peaks at 2523 ms with a value of 387 N/m (450 N/m in the experiment) which is followed by a peak of F_2 with 288 N/m (340 N/m in the experiment) at 2737 ms (Figure 4c). Residual forces of F_1 and F_2 were found to be similar to the experiment with values of 227 and 226 N/m respectively. Very good agreement has also been observed for F_3, F_4, F_5 and F_6 in terms of peak forces (172, 172, 108 and 51 N/m) the time of the peak (2864, 3070, 2912 and 3043 ms) and residual force values (116, 134, 65 and 43 N/m).

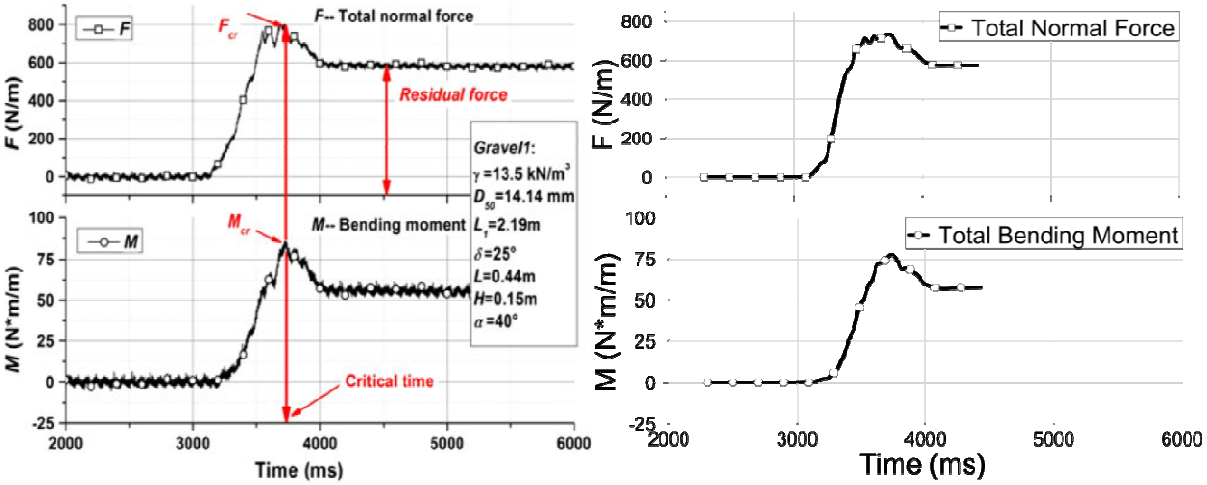

Figure 5. **Time history of total normal force and bending moment, test L44-H15-α40°: model (right) and experiment (Jiang & Towhata 2013) (left)**

Total normal force and bending moment

By considering the normal force on each part of the wall (F_i) and the distance between the centroid of the wall's parts and bottom of the retaining wall (h_i), the total normal force (F) and bending moment (M) can be calculated as follows:

$$F = \sum_{i=0}^{6} F_i \tag{3}$$

$$M = \sum_{i=0}^{6} F_i \, h_i \tag{4}$$

For the total normal force (Figure 5), the model fairly agrees with the experiment in terms of the peak force (735 N/m), peak time (3733 ms) and residual total force (576 N/m). The bending moment results (Figure 5) from the model also agrees with the experiment having a maximum bending moment of 80 N*m/m and peaking at the same time of the total force peak (3733 ms).

DISCUSSION

Comparing spherical to clumped particles, the use of clumps was preferred over spherical particles. The use of clumps led to controlling rotational velocity which was reduced by 70% leading to a better representation of the final deposition and force distribution closer to the experimental values.
In addition, by quantitative comparison with experimental results, good agreement has been observed in terms of the peak force on each part of the wall, the time of the peak and the residual force at the end of the test. Comparing impact forces, we have observed a non-linear distribution on different parts of the wall. In particular, the force at the toe of the wall is sometimes smaller than the one on the segment above. According to Jiang & Towhata (2013), this might be due to an arching effect forming an arch-like protective layer on segment 1 of the wall resulting in a non-linear distribution of forces with depth. Such a layer is also thought to affect the residual force values. For the model, to some extent, arching was observed to be present in the model, especially for residual forces of F1-F2 and F3-F4 which might be due to the force chain distributions and particles shape arrangement behind the wall. Force chains are strongly depending on the particles position and orientation with respect to the wall. The distribution of contact forces on the wall, and consequently the arching, is expected to be different from one test to another, even if conducted in the same initial conditions. It is thought that the forces measured on each segment of the wall are extremely variable. As a consequence, matching between numerical simulations and experiments should mainly concern the total force on the wall rather than on each segment. This variability should be investigated in future work, with investigations at the particle scale.

CONCLUSION

We have numerically studied the impact behavior of dry granular flow made of clumped particles (resembling gravel particles) against a segmented rigid wall. The numerical model has been calibrated considering the shape of the particle and the available experimental data of flow thickness. The model has been validated for impact force measurements against the wall. As a result, the model can be used to study impact against other types of structures (e.g. a flexible structure made of net element). Arching effect and forces variation (for the same test) on different parts of the wall depending on the initial arrangement at the beginning of the test are to be investigated.

ACKNOWLEDGEMENTS

The research leading to these results has received funding from the People Programme (Marie Curie Actions) of the European Union's Seventh Framework Programme FP7/2007-2013/ under REA grant agreement n° 289911.

REFERENCES

Azana, E., Chevor, F., Moucheront, P. 1999. Experimental study of collisional granular flows down an Inclined plane. *Journal of Fluid Mechanics*. 400, 199 – 227.

Chambers, J. M. Hastie, T. J. (1992): Statistical models in S, Wadsworth & Brooks/Cole, Pacific Grove, California, 1992.

Cundall, P.A., Strack, O.D.L. 1979. A discrete numerical model for granular assemblies. *Géotechnique*. 29(1), 47–65.

Faug. T., Beguin. R., Benoit C. 2009. Mean steady granular force on a wall over-flowed by free-surface gravity-driven dense flows. *Phys. Rev. E*, 80, 021305.

Ghaisas, N., Wassgren, C.R., Sadeghi, F. 2004. Cage Instabilities in cylindrical roller bearings. *Journal of Tribology*. 126(4): 681–689.

Guasti, G., Volkwein, A., Wendeler, C. 2011. Design of flexible debris flow barriers. In: Genevois, R.; Hamilton, D.L.; Prestininzi, A. (Eds) *5th International Conference on Debris-Flow Hazard. Mitigation, Mechanics, Prediction and Assessment. Padua, Italy, 14-17 June 2011*. 1093-1100.

Jakob, M., Hungr, O. 2005. Debris-flow hazards and related phenomena, Chichester: Springer.

Jiang, Y., Towhata, I. 2013. Experimental study of dry granular flow and Impact behavior against a rigid retaining wall. *Rock Mechanics and Rock Engineering* 46(4): 713-729.

Kishi, N., Ikeda, K., Konno, H., Kawase, R. 2000. Prototype Impact test on rockfall retaining walls and Its numerical simulation. *Proceedings of Structures under Shock and Impact IV, Cambridge, England*. 351-360.

Nicot, F., Cambou, B., Mazzoleni, G. 2001. Design of rockfall restraining nets from a discrete element modeling. *Rock Mech Rock Eng*, 34(2): 99–118.

Schwager, T., Pöschel, T. 2007. Coefficient of restitution and linear–dashpot model re-visited. *Granular Matter*. 9(6): 465–469.

Silbert, L. E., Erta¸s, D., Grest, G. S., Halsey, T. C., Levine, D., and Plimpton, S. 2001. Granular flow down an Inclined plane: Bagnold scaling and rheology. *Phys. Rev. E*, 64, 051302.

Šmilauer, V., Catalano, E., Chareyre, B., Dorofeenko, S., Duriez, J., Gladky, A., Kozicki, J., Modenese, C., Scholtès, L., Sibille, L., Stránský, J., Thoeni, K. 2010. Yade documentation (V. Šmilauer, Ed.), the Yade project, 1st Ed., 2010. Http://yade-dem.org/doc/.